Interactions of Inorganic Phosphate and Sulfate Anions with Collagen

Edward L. Mertz* and Sergey Leikin

National Institute of Child Health and Human Development, National Institutes of Health, Department of Health and Human Services, Building 9, Room 1E125, Bethesda, Maryland 20892-0924

Received June 10, 2004; Revised Manuscript Received August 12, 2004

ABSTRACT: We use direct infrared measurements to determine the number of binding sites, their dissociation constants, and preferential interaction parameters for inorganic phosphate and sulfate anions in collagen fibrils from rat tail tendons. In contrast to previous reports of up to 150 bound phosphates per collagen molecule, we find only 1−2 binding sites for sulfate and divalent phosphate under physiological conditions and ∼10 binding sites at low ionic strength. The corresponding dissociation constants depend on NaCl concentration and pH and vary from ∼50 μM to ∼1−5 mM in the physiological range of pH. In fibrils, bound anions appear to form salt bridges between positively charged amino acid residues within regions of high excess positive charge. In solution, we found no evidence of appreciable sulfate or phosphate binding to isolated collagen molecules. Although sulfate and divalent phosphate bind to fibrillar collagen at physiological concentrations, our X-ray diffraction and in vitro fibrillogenesis experiments suggest that this binding plays little role in the formation, stability and structure of fibrils. In particular, we demonstrate that the previously reported increase in the critical fibrillogenesis concentration of collagen is caused by preferential exclusion of "free" (not bound to specific sites) sulfate and divalent phosphate from interstitial water in fibrils rather than by anion binding. Contrary to divalent phosphate, monovalent phosphate does not bind to collagen. It is preferentially excluded from interstitial water in fibrils, but it has no apparent effect on critical fibrillogenesis concentration at physiological NaCl and pH.

Inorganic phosphate and sulfate anions are present in animal and human extracellular fluids at 1−3 mM concentrations, and they appear to play an important role in formation and properties of extracellular matrix. They affect collagen fibrillogenesis (*1*), interactions involving other matrix components (e.g., binding of glucosaminoglycans to collagen fibrils (*2*)), and mechanical properties of the matrix (*3*). Tribasic and dibasic forms of phosphate are also major components of hydroxyapatite crystals. Formation of these crystals within a network of collagen fibrils gives bone, dentin, enamel, and other mineralized tissues their unique properties. Interactions of ionic components of hydroxyapatite with collagen at surfaces and inside highly hydrated fibrils are, thus, likely to influence matrix mineralization and properties of mineralized tissues (*4*, *5*).

Despite their obvious importance and frequent utilization of phosphate as a buffer in biochemical studies of collagen, the underlying interactions of phosphate and sulfate with collagen fibers have so far remained largely unclear. For instance, these anions were shown to slow collagen fibril formation (*1*, *6*) and increase critical fibrillogenesis concentration (*7*). But, it was not determined whether these effects were caused by anion binding or other interactions. Even the number of bound anions was not firmly established. Some authors observed binding of ∼6 phosphates per collagen molecule at 100 mM NaCl and ∼20 phosphates at low NaCl (*5*), while others claimed up to 150 phosphates bound at 0.16 M KCl (*4*). Furthermore, we found no published values of the corresponding binding or dissociation constants and no studies distinguishing different protonation forms of phosphate (which may have different interactions with collagen).

To resolve these issues, we investigated interactions of sulfate and different protonation forms of phosphate with collagen fibrils by infrared spectroscopy, small-angle X-ray diffraction, and collagen solubility measurements. Here we report the number of binding sites for different anions and the corresponding dissociation constants. We describe the dependencies of these values on pH and NaCl concentration and suggest possible locations of the binding sites. We demonstrate that phosphate and sulfate anions not bound at these sites are preferentially excluded from interstitial water in fibrils and estimate the corresponding partition coefficients. We show how different anions affect fibril formation and structure and discuss which interactions are responsible for the observed effects.

MATERIALS AND METHODS

Solutions. Solutions were prepared from sodium salts Na_2HPO_4, NaH_2PO_4, Na_2SO_4, NaCl, and NaOH of 99.9+% purity (Aldrich) with HEPES[1] or MES buffers of 99+% purity (Aldrich) in deionized water and titrated to desired pH = 5.5−9 with concentrated NaOH.

* Corresponding author. E-mail: mertze@mail.nih.gov. Tel: (301) 402-4699. Fax: (301) 402-0292.

[1] Abbreviations: EDTA, ethylenediaminetetraacetic acid; FTIR, Fourier transform infrared; HEPES, 4-(2-hydroxyethyl)piperazine-1-ethanesulfonic acid; IR, infrared; MES, 2-(*N*-morpholino)ethanesulfonic acid; NEM, *N*-ethylmaleimide; PMSF, phenyl methyl sulfonyl fluoride; *R*, molar gas constant; RTD, resistance temperature detector; Tris, tris-(hydroxymethyl)aminomethane.

10.1021/bi048788b
Published on Web 11/05/2004

Tail Tendons. Frozen tails of 6-week-old rats were purchased from Pel-Freez Biologicals and stored at −80 °C. Tendons were excised, washed, and stored in 3.5 M NaCl, 10 mM Tris, 20 mM EDTA, 2 mM NEM, 1 mM PMSF, pH 7.5, at 4 °C. Prior to FTIR measurements, tendons were washed in 20 mM NaCl, 10 mM HEPES, pH 7.5, for a few hours at 25 °C. For some experiments, crystalline organization of collagen in tendon was disrupted by overnight equilibration in 0.2 M Na-phosphate, 1M glycerol, pH 7.5, at 4 °C, by 0.5−3 h equilibration in 0.03−0.5 M acetic acid at 25 °C, or both.

Infrared Spectroscopy. A small fiber was separated with needlepoint tweezers from a tendon soaked in 20 mM NaCl, 10 mM HEPES, pH 7.5, solution, stretched, covered by a droplet of the soaking solution, sandwiched between two ZnSe infrared windows (13 mm × 2 mm disks), and sealed by a thin layer of high-vacuum Teflon grease around the outer perimeter of the windows. The top window was fitted with inlet and outlet ports for exchanging solution. The sandwich was mounted into a specially designed flow cell the temperature of which was monitored by a RTD probe and controlled by Peltier elements to within 0.1 °C (US patent pending). The mounted sample was flattened to the desired optical path length (3−10 μm), washed with plenty of the desired solution, and annealed by several heating and cooling cycles between 5 and 45 °C. Typical final dimensions of the flattened fiber were ∼5 mm in length, ∼50−150 μm in width, and 3−10 μm in thickness. The optical path length (sample thickness) was measured from interference fringes in the spectrum of the bathing solution from 4000 to 7000 cm^{-1} (*8*). The measurements performed on two sides of each fiber used for experiments were consistent within 0.1 μm.

This setup enabled us to perform complete exchange of the bathing solution within several seconds and to set highly accurate and stable optical path length, which remained the same (within 0.01 μm measurement accuracy) for at least a month and after multiple solution changes. The variation of sample absorbance with time was less than 0.0002 absorbance units (au) during each experiment and less than 0.0005 au within a month, allowing us to perform highly accurate and reproducible measurements of difference absorption spectra.

Fourier transformed infrared (FTIR) spectra were collected in the 700−7000 cm^{-1} range with a Continuum infrared microscope (Thermo Nicolet Corp., Madison, WI) equipped with a narrow-band MCT/A detector and 15× Reflachromat IR objective/condenser. The microscope was attached to a Nexus 670 FTIR spectrometer equipped with a KBr beam splitter (Thermo Nicolet Corp.). The infrared beam was focused onto a rectangular spot within the fiber (typically 150 μm long) the position of which was controlled visually through the microscope eyepieces within ∼1 μm accuracy. Each spectrum was collected by accumulation of 300 interferometer scans at 4 cm^{-1} resolution and averaged over 3−10 runs. Spectral changes caused by variation in the bathing solution typically occurred within 15 min for acid-treated tendons and ∼120 min for untreated tendons. The final spectra were recorded after the equilibration was complete and no further spectral changes were observed.

Structural Organization of Collagen Fibers. For interpretation of our data, we distinguish three primary structural levels in hierarchical organization of macroscopic collagen fibers (e.g., see ref *9* and references therein). We refer to *microfibrils* as the smallest microscopic structural units, which consist of only several molecules in diameter (e.g., the Smith microfibril (*10*)). We refer to *fibrils* as microfibril assemblies with correlated lateral positions and well-defined axial stagger of the molecules. Finally, we refer to *fibers* as loosely packed bundles of fibrils the lateral and axial positions of which are not correlated.

To estimate the volume fractions of collagen (θ_c), interstitial water inside collagen microfibrils (θ_{wc}), and essentially bulk water filling defects within fibrils and voids between fibrils (θ_{wb}) from the IR spectra, we used several different methods: (i) We determined $\theta_{wc} + \theta_{wb}$ by comparing the observed IR spectrum of the sample in the 3000−3600 cm^{-1} range with the reference spectrum of water. We then recalculated θ_c and θ_{wc} from identity

$$\theta_c + \theta_{wc} + \theta_{wb} = 1 \quad (1)$$

and from the volume ratio for fully solvated noncrystalline rat tail tendon fibers

$$\theta_{wc}/\theta_c \approx 1.2 \quad (2)$$

estimated from Raman and X-ray measurements and water uptake by dehydrated tendon fibers (e.g., see refs *11*−*13*). The accuracy of this approach was limited by the distortion of water IR spectrum due to altered structure of interstitial water inside collagen microfibrils. (ii) We collected spectra from several fibers that were treated differently prior to being assembled in the IR cell. Some of the samples appeared to have a minimal amount of bulk water. For these samples, we estimated θ_c as ∼0.45 and used them to calibrate the intensity of nondichroic collagen IR absorption bands at 1082 and 1033 cm^{-1}. We used the intensities of these bands to determine θ_c in other samples and recalculated θ_{wc} and θ_{wb} from eqs 1 and 2. Here the accuracy was limited by the assumption that the calibration samples contained no bulk water voids and were fully solvated at the same time. (iii) Finally, we subtracted scaled IR spectra of the samples with minimal bulk water from the IR spectra of more porous samples containing substantial bulk water voids. The scaling factors were adjusted until the intensities of the 1082 and 1033 cm^{-1} bands were matched and the bulklike spectrum of water in the voids was obtained. From scaling of the void water spectrum with respect to reference water spectrum, we determined θ_{wb} and recalculated θ_c and θ_{wc} from eqs 1 and 2. From comparison of the results obtained by all three methods, we estimated that the accuracy of the measurement of θ_c and θ_{wc} was $\sim 0.1\theta_c$ and $0.1\theta_{wc}$ correspondingly. The accuracy of the measurement of θ_{wb} was $\sim 0.2\theta_{wb}$ in porous samples ($\theta_{wb} \approx 0.3$), and it was poorly defined in densely packed fibers with $\theta_{wb} < 0.1$.

X-ray Diffraction. Phosphate−glycerol-treated tendons washed in 20 mM NaCl, 10 mM HEPES, pH 7.5 (see Tail Tendons subsection), were equilibrated in 0−5 mM Na-phosphate, 3 mM HEPES at pH 6.8 and pH 8.2 at 20 °C for a week with 3−4 exchanges of the equilibrating solution. Tendon fibers from each solution were folded into a ∼5 mm long and 1 mm thick sample. Each sample was sealed in a specially designed cell with a small amount of the solution and placed into a FR590 X-ray diffractometer (Enraf Nonius) where it was maintained at 20 °C during the measurement.

The diffractometer was optimized for midangle X-ray diffraction with the range of reciprocal space vectors q from 0.1 to 1 Å^{-1} and reciprocal space resolution of ~0.02 Å^{-1}. Details of the design of X-ray cells and temperature controllers were described in ref *14*. The diffraction patterns were recorded on FUJIFILM MS imaging plates and scanned on a FUJIFILM FLA-3000 (FUJI Medical Systems) scanner.

Purified, Pepsin-Treated Collagen. Purified, pepsin-treated collagen was prepared by pepsin (Calbiochem) digestion of rat tail tendons in 0.5 M acetic acid (1:10 pepsin/tendons added in two doses separated by 24 h) followed by two rounds of salt precipitation (1 M NaCl in 0.5 M acetic acid). The final precipitate was resuspended in 2 mM HCl (pH 2.7), dialyzed against excess 2 mM HCl, mixed 1:1 with 20 mM sodium phosphate, 0.26 M NaCl (pH 7.5 after mixing), and equilibrated at 32 °C overnight. The resulting collagen fibrils were spun down, resuspended in 50 mM acetic acid, dialyzed against excess 50 mM acetic acid overnight, freeze-dried under vacuum, and stored at 4 °C.

For fibrillogenesis experiments, pepsin-treated collagen was dissolved in 2 mM HCl and additionally purified by two rounds of fibrillogenesis in 130 mM NaCl, 10 mM HEPES (pH 7.5) at 0.2 mg/mL collagen concentration. Resulting fibrils were spun down, resuspended in 2 mM HCl, and extensively dialyzed, and collagen concentration in the final stock solution was adjusted to 0.8 mg/mL.

In Vitro Fibrillogenesis. Aliquots of purified, pepsin-treated collagen solution were mixed on ice with buffer and salt stocks to produce final solutions of 0.2 mg/mL collagen, 0−30 mM Na-sulfate or Na-phosphate, 130 mM NaCl, 10 mM HEPES at pH 6.8, 7.5, and 8.2. The samples were sealed in 0.5 mL vials and thermostated at 32 ± 0.2 °C overnight. Control measurements of solution turbidity produced typical S-shaped curves (*1*), indicating that fibril assembly was complete within several hours. The fibrils were spun down for 10 min at 20 000*g*, 32 °C; supernatants were removed and mixed 200:1 with 6% Brij-35. Supernatants were handled with pipet tips and vials rinsed in 0.03% Brij-35 to reduce collagen adsorption.

Collagen concentration in the supernatant was determined from the difference in the circular dichroism (CD) spectra of native and denatured protein at 30 °C in a quartz microcell with 10 mm optical path length sealed by a Teflon stopper (Starna). The spectra were collected in a Jasco-810 spectropolarimeter equipped with thermoelectric temperature controller (Jasco Inc) and averaged over 25 scans. Collagen was denatured by heating the cell to 60 °C for 5 min followed by cooling and thermostating at 30 °C for 5 min. Time-resolved measurements confirmed that denaturation was complete and no detectable renaturation occurred. The method was calibrated by using reference collagen solutions (2−30 μg/mL), and its sensitivity and accuracy were estimated as ~1 μg/mL of collagen.

Alternatively, collagen concentration was measured by mixing supernatant aliquots with bovine serum albumin (BSA, Sigma), labeling with monoreactive Cy5 (Amersham) as described previously (*15*) and separating on 3−8% (gradient) precast Tris−acetate gels (Invitrogen) under standard reducing conditions. The gels were analyzed in a FUJIFILM FLA-5000 fluorescence scanner (FUJI Medical Systems). Intensities of collagen α1(I) and α2(I) bands were normalized to the BSA bands and compared with corresponding normalized intensities of reference solutions. The sensitivity and accuracy of this method were estimated as <0.1 μg/mL and ~25%. These and CD measurements produced the same results for the same solutions.

THERMODYNAMIC ANALYSIS

Phosphate and Sulfate Binding and Partitioning. In our analysis, we followed an established tradition of separating strong binding of solutes (here phosphate or sulfate anions) at specific binding sites and weak preferential interactions of "free" solutes with proteins (*16*−*19*). Within this approach, strong (specific) binding means that the number of potential binding sites per protein is limited and a substantial fraction of them can be occupied by bound solutes at relevant solute concentrations. The preferential interactions may involve, for example, exclusion or inclusion of solutes into protein solvation shells in exchange for water molecules. However, in contrast to strong binding, the number of such solutes is proportional to their concentration in the surrounding solution. Therefore, it is convenient to refer to such solutes as "free" rather than bound yet preferentially localized at protein surface.

For analysis of the IR data on phosphate or sulfate concentration in collagen fibrils, we also assumed that strong binding of these anions to collagen can be described by a simple binding isotherm with noninteracting binding sites and a single effective dissociation constant (K_D). Then the total concentration of anions in a fibrillar sample (per unit of sample volume) is given by

$$X_{smpl} = \underbrace{c_b \frac{X}{X + K_D}}_{\text{bound anions}} + \underbrace{\alpha X}_{\text{"free" anions}} \qquad (3)$$

where X is the anion concentration in the bathing solution, c_b is the concentration of anion binding sites per unit fiber volume, and α is the apparent penetration coefficient for "free" anions. The values of c_b and α are related to the composition of the sample in the IR beam as follows

$$c_b = n\frac{\theta_c}{V_c} \qquad \text{and} \qquad \alpha = p\theta_{wc} + \theta_{wb} \qquad (4)$$

where n is the number of binding sites per collagen molecule in a fiber and $V_c \approx 210$ L/mol is the molar volume of collagen. The partition coefficient p determines to what extent "free" anions are preferentially excluded ($p < 1$) or included ($p > 1$) into interstitial water (*17*, *18*).

The values of c_b, K_D, and α were determined directly by fitting of the measured dependence of X_{smpl} on X (cf. Figures 3 and 4) to eq 3, and the values of n and p were recalculated by using θ_c, θ_{wc}, and θ_{wb} determined as described in Materials and Methods.

To find the pH dependence of dibasic phosphate dissociation constant from measurement of the pH dependence of $X_{smpl} = [HPO_4^{2-}]_{smpl}$ at constant phosphate concentration in solution, $[H_2PO_4^-] + [HPO_4^{2-}]$, we used the fact that c_b and α for dibasic phosphate appear to be pH-independent (Table 1). Then,

Table 1: Binding and Preferential Interaction Parameters Obtained by Fitting of Anion Concentrations Accumulated in a Solvated Tendon (cf. Figures 3 and 4) to Eqs 3 and 4[a]

		pH 6.8			pH 8.2	
anion	parameter	0 mM NaCl	20 mM NaCl	130 mM NaCl	0 mM NaCl	130 mM NaCl
$H_2PO_4^{1-}$	K_D, mM	*b*	*b*	*b*		
	n, mol/mol	*b*	*b*	*b*		
	α	0.46 ± 0.05	0.40 ± 0.05	0.28 ± 0.05		
	p	0.45 ± 0.12	0.31 ± 0.14	≤0.17		
HPO_4^{2-}	K_D, mM	0.034 ± 0.003	1.7 ± 0.15	1.9 ± 1	0.37 ± 0.04	*b*
	n, mol/mol	9.9 ± 0.2	8.9 ± 0.5	1.7 ± 0.5	8.6 ± 0.3	*b*
	α	0.31 ± 0.02	0.28 ± 0.02	0.34 ± 0.03	0.38 ± 0.03	
	p	≤0.24	≤0.17	≤0.31	0.23 ± 0.15	
SO_4^{2-}	K_D, mM	0.15 ± 0.05	4 ± 0.7		0.5 ± 0.1	
	n, mol/mol	11.1 ± 1	11.1 ± 1		10.3 ± 0.5	
	α	0.46 ± 0.05	0.32 ± 0.03		0.48 ± 0.04	
	p	0.45 ± 0.12	≤0.26		0.51 ± 0.12	

[a] All data are for the *same* tendon sample at 32 °C. The dissociation constant for bound anions (K_D) and the apparent penetration coefficient for "free" anions (α) were obtained directly from fitting. The number of binding sites per collagen molecule (*n*) and the partition coefficient for "free" anions in interstitial water in fibrils (*p*) were calculated from eq 4 based on the fit parameters and volume fractions ($\theta_c = 0.33 \pm 0.03$, $\theta_{wc} = 0.40 \pm 0.04$, and $\theta_{wb} = 0.27 \pm 0.06$) determined for this sample as described in Materials and Methods. All indicated errors are associated with the fitting and the uncertainties in the volume fractions. The sample-to-sample variation was evaluated as ~50% and ~10% for K_D and *n*, respectively, at pH 6.8, 0 mM NaCl. [b] Linear concentration dependence with no appreciable binding was observed, indicating that $n < 0.5$ or $K_D > 50$ mM.

$$K_D(\mathrm{pH}) = \frac{c_b X}{X_{smpl} - \alpha X} - X, \quad \text{where}$$

$$X = \frac{[HPO_4^{2-}] + [H_2PO_4^{-}]}{1 + 10^{7.2-\mathrm{pH}}} \quad (5)$$

and we used the fact that the p*K* for dibasic−monobasic phosphate titration is 7.2.

To describe the observed variation of the dissociation constant with pH, we assumed that at high pH $K_D = K_D^0$ while at low pH $K_D = K_D^H$, where K_D^0 and K_D^H are the dissociation constants for the unprotonated and protonated forms of the binding sites, correspondingly. Then, the pH dependence of the average dissociation constant is

$$K_D = \frac{K_D^0 + K_D^H 10^{pK_X - pH}}{1 + 10^{pK_X - pH}} \quad (6)$$

provided that protonation of binding sites in the presence of bound anions can be described by a single p*K* ($pK = pK_X$). On the basis of experimental observations, we neglected binding of protonated anions ($H_2PO_4^-$ and HSO_4^-).

Collagen Solubility. For analysis of collagen solubility data, we assumed that at small anion concentration *X*, the dependence of collagen solubility *s* on *X* is given by (*17*, *18*, *20*−*22*)

$$\ln\left(\frac{s}{s_0}\right) = \kappa_X X - n \ln\left(1 + \frac{X}{K_D}\right) + n' \ln\left(1 + \frac{X}{K_D'}\right) \quad (7)$$

where s_0 is collagen solubility at $X = 0$, n' is the number of anion binding sites per collagen molecule in solution, and K_D' is the effective dissociation constant for these sites. The coefficient

$$\kappa_X = \frac{1}{RT}\left[\frac{\partial(\tilde{\mu}_c' - \tilde{\mu}_c)}{\partial X}\right]_{P,T,X=0} \quad (8)$$

is defined by the change in the chemical potential of collagen, $\tilde{\mu}_c' - \tilde{\mu}_c$, upon transfer from solution into aggregate in the absence of strongly bound anions ($n = n' = 0$). It is associated with weak preferential interactions of collagen with water and anions, that is, a difference in the net surface deficit (excess) of anions near collagen molecules in fibrils and in solution (*17*, *18*, *20*−*22*).

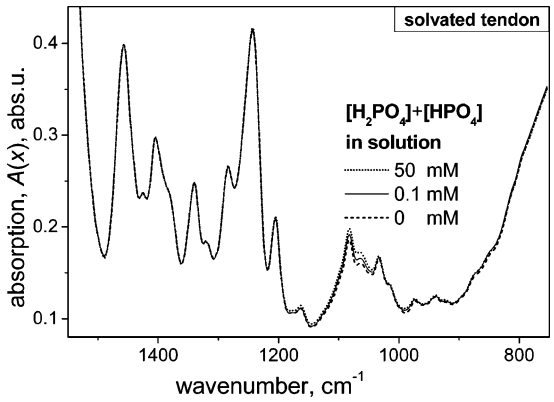

FIGURE 1: Infrared absorption spectra of a 7-μm-thick solvated rat tail tendon equilibrated at different phosphate concentrations (3 mM HEPES, pH 6.8, 32 °C). Spectral changes occur only in the 1200−900 cm^{-1} region of phosphate absorption (cf. Figure 2).

RESULTS

Difference IR Spectra. To measure small changes in infrared (IR) spectra of solvated collagen fibers due to phosphate and sulfate binding, we used an FTIR microscope with a specially designed flow cell described in Materials and Methods. This setup enabled us to keep the IR beam focused on the same region of a solvated fiber, to prevent the beam from passing through the surrounding solution, and to establish a precise, constant beam path length inside the sample. The resulting IR spectra of the same solvated collagen fiber measured at different phosphate concentrations are shown in Figure 1.

The absence of changes in collagen absorption bands from 1200 to 1500 cm^{-1} indicates that the addition of phosphate does not induce any changes in the structure of fibrillar collagen. The barely detectable (<0.5%) changes in the librational band of water below 850 cm^{-1} (both in fibers and bulk solution) are consistent with expulsion of water

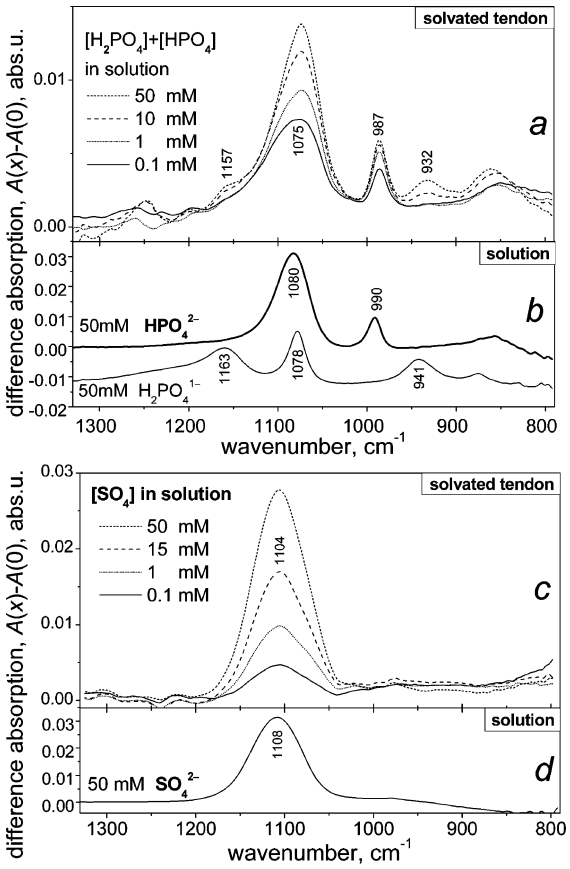

FIGURE 2: Difference infrared spectra, $A(X) - A(X=0)$, of a solvated rat tail tendon at different phosphate (a) and sulfate (c) concentrations X (3 mM HEPES, pH 6.8, 32 °C). The spectra are similar to the difference spectra of phosphate (b) and sulfate (d) in solution. Integral intensities of the 1104, 987, and 932 cm^{-1} bands were used to determine the concentrations of sulfate, dibasic phosphate, and monobasic phosphate in fibers, respectively.

from the volume occupied by anions and otherwise unchanged collagen hydration. Similar conclusion of no changes in collagen hydration can also be drawn from the absence of changes in the hydration-sensitive (*23*) collagen absorption bands, as well as minute (<0.5%) changes in water bands at 3000−3700 cm^{-1}. The only significant (up to ~10%) spectral changes in Figure 1 are seen in the 900−1200 cm^{-1} region and are entirely consistent with absorption of phosphate, which penetrated inside collagen fibrils.

High reproducibility of these measurements allowed us to perform accurate subtraction of the fiber spectrum at zero ion concentration. The corresponding difference spectra at different sulfate concentrations (Figure 2) are similar to the spectrum of sulfate in solution (Figure 2), except for a small frequency shift apparently related to different hydrogen bonding environment of sulfate inside collagen fibrils. Likewise, difference spectra at different phosphate concentration appear to be superimpositions of $H_2PO_4^{1-}$ and HPO_4^{2-} absorption bands (cf. Figure 2). We further confirmed such assignment by isotopic substitution ($D_2PO_4^{1-}$ and DPO_4^{2-} in D_2O), which resulted in similar frequency shifts in collagen fibrils and in solution.

On the basis of this interpretation, we used the 1104 cm^{-1} band for sulfate, 987 cm^{-1} band for dibasic phosphate, and 932 cm^{-1} band for monobasic phosphate to measure concentrations X_{smpl} of these ions inside collagen fibrils from the difference spectra. Specifically, $X_{smpl} = X_{ref}(I_{smpl}/L_{smpl})/(I_{ref}/L_{ref})$, where X_{smpl} is the anion concentration per unit volume of the fibrillar sample and I_{smpl} and L_{smpl} are the integral intensity of the corresponding IR band and the beam path length in the sample. X_{ref}, I_{ref}, and L_{ref} are the anion concentration, IR band intensity, and beam path length in a reference anion solution. (Alternative determination of phosphate concentration based on decomposition of the broadened peak between 1200 and 1000 cm^{-1} into the 1080 cm^{-1} band of HPO_4^{2-} and 1078 and 1163 cm^{-1} bands of $H_2PO_4^{1-}$ produced similar results).

Phosphate and Sulfate Binding and Partitioning. As discussed in Materials and Methods (Structural Organization of Collagen Fibers), three different subpopulations of sulfate and phosphate might contribute to the total measured concentration: (i) anions bound to collagen, (ii) "free" anions dissolved in interstitial water inside collagen fibrils, and (iii) anions in bulk aqueous solution filling the voids between fibrils and structural imperfections of the sample. Relative contributions of these subpopulations are proportional to the volume fractions of collagen (θ_c), interstitial water (θ_{wc}), and bulk water in defects within fibrils and in voids between fibrils (θ_{wb}), correspondingly. These volume fractions varied from sample to sample and were determined from analysis of water and collagen contributions to the IR spectra as described in Materials and Methods.

The dependence of sulfate concentration in the sample X_{smpl} on its concentration in the bathing solution X observed at pH 8.2 and pH 6.8 in the same sample is shown in Figure 3. The initial steep rise of X_{smpl} is substantially larger than the sum of the contributions from interstitial water and void fractions, $(\theta_{wc} + \theta_{wb})X$, expected in the absence of interactions of sulfate with collagen (dotted line). Thus, the observed rapid accumulation of sulfate appears to be caused by its binding to collagen. All binding sites appear to be filled when sulfate concentration in the surrounding solution exceeds several millimolar. The subsequent linear increase in X_{smpl} is consistent with accumulation of sulfate in interstitial water and voids. However, the slope of this dependence is smaller than expected in the absence of interactions of sulfate with collagen, suggesting preferential exclusion of sulfate from interstitial water.

To describe these effects quantitatively, we assumed that (a) sulfate binding can be described by a simple binding isotherm with noninteracting binding sites and a single dissociation constant K_D, (b) the molal concentration of sulfate in voids is the same as that in the bathing solution, and (c) molal concentration of sulfate in interstitial water is proportional to the bulk concentration with the partition coefficient p ($p < 1$ corresponds to ion exclusion from interstitial water). The corresponding isotherm (eqs 3 and 4) was fitted to the data as shown in Figure 3. The fitted values of the number of binding sites per collagen molecules, n, the dissociation constant, K_D, the apparent anion penetration coefficient, $\alpha = p\theta_{wc} + \theta_{wb}$, and the partition coefficient for interstitial water, p, are listed in Table 1. Figure 3 graphically illustrates the separation of total sulfate into bound and "free" (interstitial + void) fractions at pH 8.2.

Concentrations of monobasic ($H_2PO_4^{1-}$) and dibasic (HPO_4^{2-}) phosphate measured in the same sample at pH 8.2 and pH 6.8 are shown in Figure 4. The observed isotherms for dibasic phosphate are qualitatively similar to those of sulfate. The corresponding numbers of binding sites, dis-

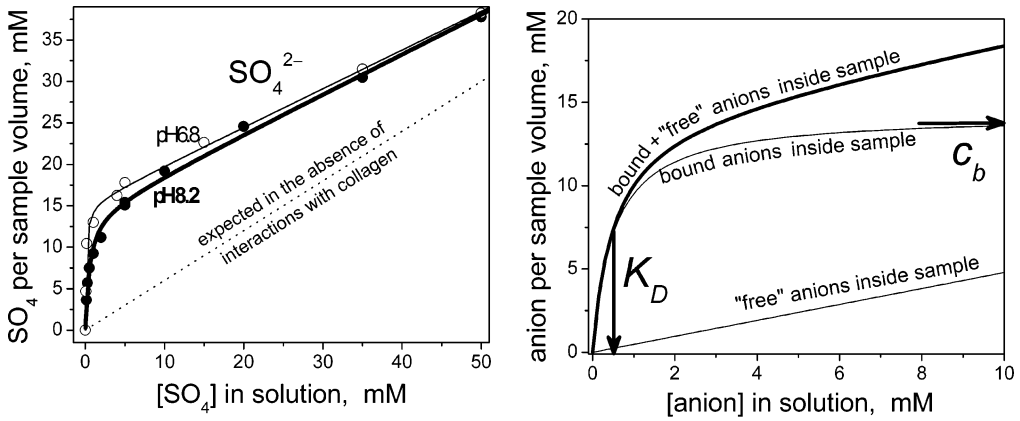

FIGURE 3: The left panel shows accumulation of sulfate inside a solvated rat tail tendon upon variation of its concentration in the bathing solution at pH 6.8 and 8.2 (3 mM HEPES, 32 °C). The solid lines are fits to eq 3. The dotted line is the concentration expected in the absence of binding and preferential interactions of anions with collagen. The slope of this line is the total volume fraction of water in tendon. The right panel shows the contributions of bound and "free" (not bound to specific sites) anions into the total concentration of sulfate inside tendon at pH 8.2. The corresponding curves were calculated from eq 3 based on the fitted values of the concentration of binding sites, c_b, their dissociation constant, K_D, and the penetration coefficient α for "free" anions (the slope of the "free" anions line).

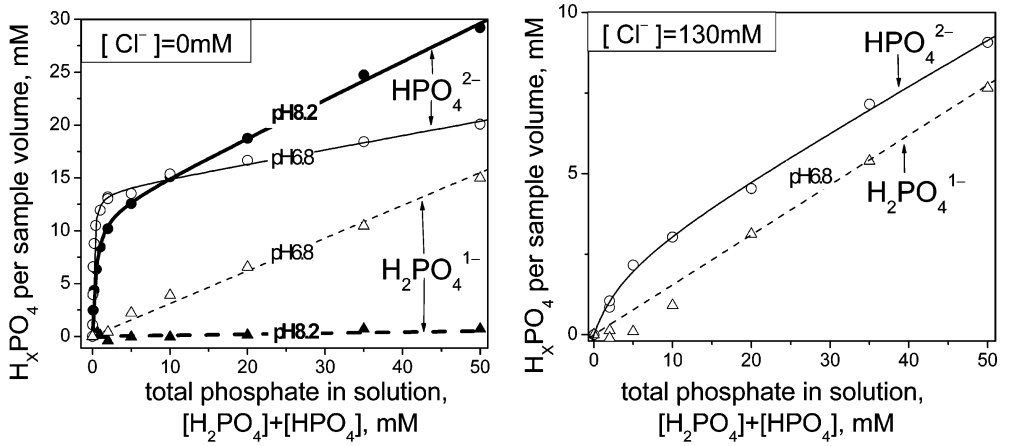

FIGURE 4: Accumulation of monobasic and dibasic phosphate in solvated tendon upon variation of phosphate concentration in 3 mM HEPES solutions (32 °C) at 0 mM NaCl, pH 6.8 and 8.2 (left), and 130 mM NaCl, pH 6.8 (right). The lines are fits to eq 3. Straight line fits suggest that monobasic phosphate does not bind to collagen in fibers. The slopes of all lines at high concentrations (in the linear regime) are smaller than the volume fraction of water in the sample, indicating that both dibasic and monobasic phosphate anions not bound to specific sites are preferentially excluded from interstitial water in fibrils.

sociation constants, and partition coefficients are also listed in Table 1.

Monobasic phosphate exhibits no appreciable binding. Like dibasic phosphate, it is partially excluded from interstitial water inside fibrils ($p < 1$). However, its partition coefficient could be estimated only at pH 6.8 when a significant fraction (71%) of total phosphate in solution was in the monobasic form. At pH 8.2, only 9% of phosphate in solution was monobasic, and no monobasic phosphate could be detected inside fibrils within the experimental error.

Effect of pH on Phosphate and Sulfate Binding and Partitioning. Comparison of the measured concentrations (Figures 3 and 4) and of the corresponding dissociation constants (Table 1) reveals substantially stronger binding of divalent anions to collagen at pH 6.8 than at pH 8.2. The binding at lower pH is enhanced due to a substantial decrease in the corresponding dissociation constants, while the number of binding sites and the partition coefficients of "free" ions appear to be pH-independent. The observed effect is qualitatively similar for sulfate and dibasic phosphate, although the change in the sulfate K_D appears to be smaller.

A more detailed pH dependence of dibasic phosphate binding is shown in Figure 5 at fixed total phosphate concentration in solution, $[H_2PO_4^{1-}] + [HPO_4^{2-}] = 0.2$ mM. Upon pH decrease from 8.8 to 5.5, the concentration of dibasic phosphate bound inside fibrils increases from about 2.5 to about 10 mM, while the concentration of dibasic phosphate in the surrounding solution decreases from 0.2 to less than 0.004 mM. Figure 5 shows the corresponding values of dibasic phosphate K_D determined from the titration curve for $[HPO_4^{2-}]_{smpl}$ by using the pH-independent values of n and α measured at pH 6.8 and 8.2 (see eq 5). The resulting pH dependence of K_D is well fitted by a simple titration curve for dibasic phosphate binding sites (eq 6) with $pK = 8.2 \pm 0.2$ (Figure 5). The extrapolated plateau values of K_D at low and high pH are $\leq$300 nM and $\sim$1 mM, that is, differ by more than 3 orders of magnitude.

Effect of Salt. We observed a profound effect of NaCl on binding of sulfate and dibasic phosphate and some effect on the partition coefficient of monobasic phosphate (see Table 1). Specifically, at pH 6.8, addition of 20 mM NaCl increased the dissociation constants of sulfate and dibasic phosphate about 30-fold while the apparent number of binding sites remained unchanged. Further addition of NaCl to 130 mM had almost no effect on the dissociation constant of dibasic phosphate. At the same time, the number of binding sites

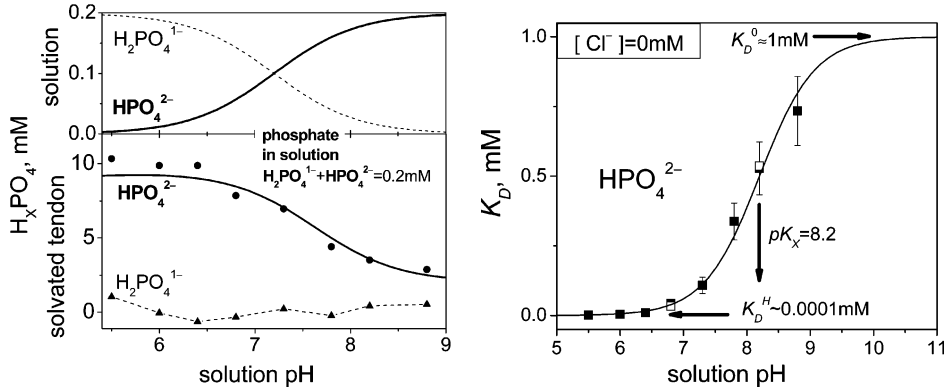

FIGURE 5: The left panel shows variation of dibasic and monobasic phosphate concentrations with pH in solution (calculated from known pK_2, top) and in tendon (measured by IR, bottom) upon equilibration in 0.2 mM total phosphate, 3 mM HEPES at 20 °C. The solid line in the bottom panel is the best fit to eqs 3−6. Only bound phosphate anions are detectable by IR in tendon at these conditions. The absence of bound monobasic phosphate at pH 5.5 suggests that pK_2 of bound phosphate is at least 3 units lower than that in solution. The right panel shows the dependence of the dissociation constant, K_D, for dibasic phosphate on pH in 3 mM HEPES at 20 °C. Solid squares are the data recalculated from the plots on the left by means of eq 5. Open squares are K_D obtained by fitting of 20 °C isotherms similar to those shown in Figure 4. The solid line is the best fit to eq 6. Note that the binding sites are protonated with p$K_X \approx 8.2$ in the presence and p$K = [8.2 - \log(K_D^0/K_D^H)] \approx 4-5$ in the absence of bound phosphate.

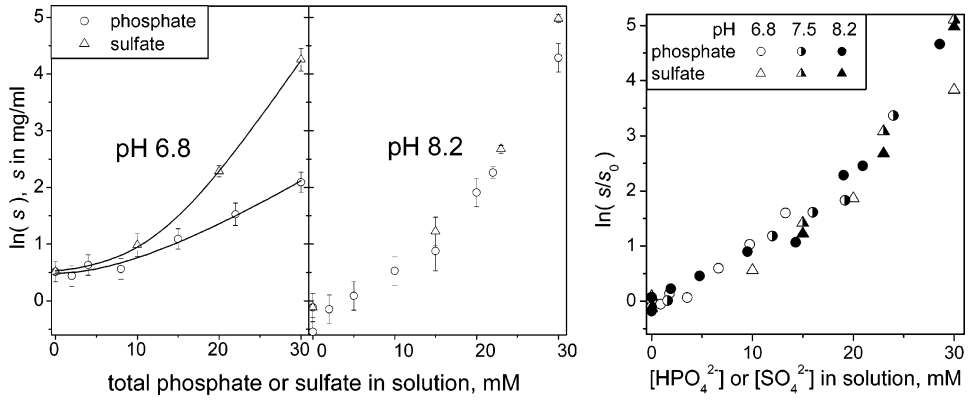

FIGURE 6: Collagen solubility vs phosphate and sulfate concentrations in 130 mM NaCl, 10 mM HEPES at 32 °C. Lines are fits to eq 7. The normalized ($\ln(s/s_0)$) solubility curves coincide for phosphate and sulfate at all pH when plotted vs concentrations of divalent anions (right panel), suggesting that monobasic phosphate has no effect on solubility.

decreased from ~10 to ~2, suggesting that at least two different types of binding sites might be present in the sample (more and less sensitive to salt). A qualitatively similar effect was observed at pH 8.2, but it was difficult to measure quantitatively due to substantially higher dissociation constants.

Effects of Temperature, Osmotic Pressure, and Tendon Crystallinity. In addition to salt and pH, collagen fiber structure is affected by temperature and osmotic pressure (*24*, *25*). However, we found that only salt and pH had a significant effect on phosphate binding. We observed no substantial changes in the dissociation constant and number of binding sites for dibasic phosphate upon fiber dehydration by up to 10% PEG and upon temperature change from 20 to 32 °C. Furthermore, within the range of sample-to-sample variation, the dissociation constant and the number of binding sites were the same in crystalline tendon fibers and in fibers the crystallinity of which was disrupted (*26*) by phosphate−glycerol or acid treatments or both (cf. Table 1).

Collagen Solubility. Addition of phosphate was found to increase fibrillogenesis lag time (*1*, *7*) and collagen solubility (*7*). Similar but weaker effect on the lag time was also observed for sulfate (*6*). To better understand the role of mono- and dibasic ionic forms of phosphate and the role of phosphate binding in collagen fibril formation, we measured the dependence of equilibrium collagen solubility on phosphate and sulfate concentrations at pH 6.8, 7.5, and 8.2. Since NaCl affects binding of dibasic phosphate and partitioning of monobasic phosphate in collagen fibrils, we chose to perform these experiments in 10 mM HEPES buffer with constant 130 mM NaCl concentration. Following the established tradition (*27*, *28*), we defined the solubility as the concentration of collagen in supernatant after overnight equilibration in the corresponding buffer at 32 °C followed by centrifugation (see Materials and Methods).

The observed dependence of the logarithm of solubility on phosphate and sulfate concentration is shown in Figure 6. The effect of phosphate is highly pH-dependent, while the effect of sulfate is not. However, when the logarithm of collagen solubility is plotted vs the concentration of dibasic phosphate, the effect appears to be pH-independent and identical to the effect of sulfate (Figure 6, right panel). Unless this is a coincidence, it appears that the increase in collagen solubility upon variation of phosphate can be attributed entirely to the action of the dibasic form of phosphate.

Fitting as well as qualitative comparison of the solubility data with eq 7 suggest that (i) the main linear trend of the observed solubility increase is caused by preferential interactions of anions with collagen, (ii) anion binding to collagen in fibrils reduces solubility and explains the observed

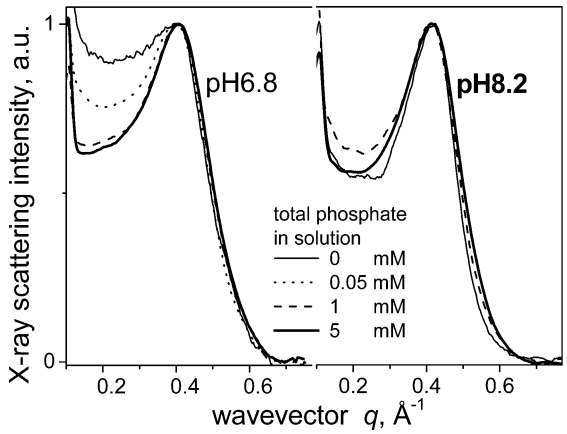

FIGURE 7: Equatorial profiles for small-angle X-ray scattering from solvated tendons at different phosphate concentrations in 3 mM HEPES, pH 6.8 and 8.2, at 20 °C. Phosphate binding does not affect the Bragg peak position at either pH, suggesting that the distance between most nearest-neighbor molecules in fibrils remains the same. At pH 6.8, lateral packing of the molecules at larger distance scales is disrupted, as indicated by appearance of a shoulder at small q without phosphate. The disappearance of this shoulder above 1 mM phosphate indicates that phosphate binding restores this packing.

deviation from linearity, and (iii) there is no appreciable anion binding to collagen in solution in the 0−50 mM concentration range. The best fit parameters based on these assumptions are $\kappa_{HPO_4^{2-}} \approx \kappa_{SO_4^{2-}} \approx 250\ M^{-1}$, $n \approx 1-2$, and $K_D \approx 5$ mM. The fitted curves are shown in Figure 6. The fitted number of binding sites, n, and the dissociation constant, K_D, in fibrils are in reasonable agreement with direct IR measurements (Table 1). However, their evaluation from collagen solubility data is less reliable. (They are responsible for only a relatively small contribution to the solubility, and their fitted values might be affected by other neglected contributions from fibrillogenesis-incapable collagen, osmotic compression of fibers by excluded ions, etc.).

Note that the dependence of the logarithm of collagen solubility on phosphate concentration observed here is in qualitative agreement with the dependence reported in ref *7*. However, collagen solubility at zero anion concentration (∼0.5−1 μg/mL) and the slope of this dependence (∼250 M^{-1}) are different from the corresponding values (∼10 μg/mL and ∼13 M^{-1}) obtained in ref *7*. The difference could be related, for example, to a different buffer system and higher purity of the collagen used in the present study (see Materials and Methods).

Fiber Structure. To evaluate the effect of bound dibasic phosphate on collagen−collagen interactions, we measured equatorial X-ray diffraction patterns from collagen fibers (Figure 7). To improve sensitivity of the measurement, we used tendon fibers of which the crystallinity was disrupted by phosphate−glycerol treatment (see Materials and Methods). To prevent compression (dehydration) of fibers due to osmotic action of excluded ions, we performed the measurements without NaCl and at phosphate concentrations below 5 mM (which should still be sufficient to saturate all binding sites, see Table 1).

Representative diffraction patterns measured at pH 6.8 and pH 8.2 at different phosphate concentrations are shown in Figure 7. The peak at $q \approx 0.42$ $Å^{-1}$ arises from quasi-hexagonal packing of molecules inside the fibrils and corresponds to the average interaxial spacing of $d_{int} = 4\pi/(q\sqrt{3}) \approx 17$ Å (*26*). The relatively large width of this peak and the absence of higher order diffraction peaks are characteristic of noncrystalline fibers and might be caused by small diameter of collagen fibrils, as well as by deviations from the ideal hexagonal packing with relatively broad distribution of interaxial spacings (*26*, *29*−*31*).

We observed no effect of pH and phosphate addition on the position of the diffraction peak within the experimental error (∼0.01 $Å^{-1}$), suggesting that the average interaxial distance between molecules inside fibrils was the same. However, we observed substantial broadening of this peak toward lower q at pH 6.8 suggesting some disruption of fibril structure (see Discussion). This broadening was reduced already by 0.05 mM phosphate and completely eliminated by 1 mM phosphate. Higher phosphate concentrations, up to 5 mM, had no additional effect on the diffraction pattern.

Interestingly, visual examination at low magnification revealed a swollen appearance of phosphate−glycerol-treated fibers equilibrated at pH 6.8 without phosphate. Subsequent addition of phosphate reduced (0.05 mM phosphate) or eliminated this visible swelling (1−5 mM), while NaCl had a substantially weaker effect.

DISCUSSION

Phosphate and sulfate anions accumulate inside collagen fibrils both as bound to collagen and as dissolved ("free") in interstitial water, which comprises ∼55% of fibril volume. We utilized IR microspectroscopy to *directly* observe this process in rat tail tendon fibers (viz., fibril bundles, see Structural Organization of Collagen Fibers in Materials and Methods), to detect differences in interaction of monobasic and dibasic phosphate with collagen, to determine the number of binding sites and the dissociation constant (K_D) for each anion, to evaluate preferential interactions of "free" interstitial anions with fibrillar collagen, and to track conformational changes in collagen backbone. We also used X-ray diffraction to study the effect of bound anions on fibril structure and measured critical fibrillogenesis concentration to find how binding and preferential interactions of "free" anions affect thermodynamics of fibrillogenesis.

Number of Binding Sites and Dissociation Constants. At physiological conditions, dibasic phosphate (HPO_4^{2-}) binds in one to two sites per collagen molecule with $K_D \approx 1-3$ mM. In contrast, monobasic phosphate ($H_2PO_4^-$) exhibits no appreciable binding. At low salt and neutral pH, the number of dibasic phosphate binding sites increases to ∼10, still characterized by a single effective $K_D \approx 50$ μM (Table 1). The observed K_D values for phosphate are highly pH-dependent. For instance, low-salt K_D decreases from ∼1 mM at pH 9 to ∼0.1 μM below pH 6 (Figure 5). The number of binding sites, the values of K_D, and the dependencies of these parameters on salt and pH are similar for sulfate.

Binding Mechanism. Relatively low water content of collagen fibrils and narrow interstitial space between collagen molecules (surface to surface separation between collagen molecules ∼5−7 Å) makes the presence of large phosphate and sulfate anions (diameter ∼6 Å) inside fibrils energetically unfavorable unless compensated by other interactions. Our data show that phosphate and sulfate binding involves direct hydrogen bonding with positively charged amino acid

residues, but the main contribution to the binding energy appears to come from electrostatics. Specifically, difference IR spectra (Figure 2) reveal 3−10 cm^{-1} frequency downshifts for the characteristic IR bands of bound anions, indicating formation of hydrogen bonds that are stronger than those with water. However, the similarity between dibasic phosphate and sulfate (rather than between two forms of phosphate) and the observed 30-fold increase in K_D at 20 mM NaCl suggest that electrostatic interactions are more important. Most likely NaCl creates an ionic atmosphere inside fibrils, screens the excess positive charge in the binding sites, and, thereby, reduces the binding free energy. (Although we cannot exclude competitive binding of Cl^- as an alternative explanation, the observed effect of NaCl would then require $K_D < 1$ mM for Cl^-, which is unlikely considering that monobasic phosphate exhibits no appreciable binding in this concentration range).

We believe that divalent anions bind at sites with excess positive charge where they form salt bridges between two positively charged amino acid residues not involved in ion pairs with negatively charged residues. This interpretation also explains why bound phosphate has $pK_2 \leq 4$ while phosphate in solution has $pK_2 \approx 6.9-7.2$ (depending on salt concentration). Indeed, bridging of two cationic groups by a divalent anion is far more energetically favorable than that by a monovalent anion. Therefore, formation of such bridges favors dibasic phosphate by shifting phosphate pK_2.

It is tempting to speculate that the observed phosphate binding and the accompanying shift in phosphate pK_2 might play an important role in matrix mineralization by helping to accumulate divalent phosphate anions necessary for formation of hydroxyapatite crystals, binding of collagen fibrils to crystal surfaces, or both.

Possible Locations of Binding Sites. Binding of polyanions at one to two sites with high excess positive charge on each collagen molecule (both in solution and in fibrils) was proposed based on collagen amino acid sequence and electron microscopy of glycosaminoglycan complexes (*32*). For lower-charge, divalent anions, we find no evidence of binding to isolated collagen molecules in solution and up to 10 binding sites per molecule inside fibrils. Thus, while divalent anion binding in fibrils might occur at the site(s) proposed in ref *32*, it must also occur at additional sites, probably associated with accumulation of excess positive charge due to staggered alignment of neighbor molecules. A qualitative illustration of the existence of highly charged regions that might contain such sites is given in Figure 8. It shows locations and the net charge of regions where pairs of closely positioned Lys^+ and Arg^+ and no Glu^- or Asp^- (on the same or opposing molecules) are likely to occur and form salt bridges with divalent anions. Additional positively charged residues in the vicinity but not in direct contact with salt bridges would further stabilize binding due to long-range electrostatic interactions. To confirm involvement of these or any other sites in divalent anion binding, more detailed studies are needed, but this is beyond the scope of the present work.

Interestingly, four of the potential binding sites contain histidine residues consistent with the observed pH dependence of phosphate K_D. Indeed, this dependence implies that most binding sites are protonated with $pK_X \approx 8.2$ in the presence of bound dibasic phosphate (Figure 5). The protonation pK of the same sites in the absence of bound phosphate should be lower by $\log[K_D^0/K_D^H]$, that is, $pK \approx 4-5$. This range of pK within highly positively charged sites is likely to be observed for histidine.

Role of Anion Binding in Fibrillogenesis. While phosphate and sulfate bind to one to two sites per collagen molecule at physiological conditions, this binding has only weak promoting effect on fibrilogenesis. Consistent with previous reports (*1*, *7*), we did not observe any substantial changes in the fibrillogenesis kinetics at physiological (1−3 mM) phosphate and sulfate concentrations (data not shown). More importantly, at these concentrations, phosphate and sulfate have only minimal net effect on critical fibrillogenesis concentration (collagen solubility) at 32 °C (Figure 6).

However, at low ionic strength, phosphate binding becomes more significant, and it begins to affect collagen−collagen interactions. For instance, pH 6.8 leads to visible swelling of fibers compared to pH 8.2. The accompanying changes in the low-angle equatorial X-ray diffraction pattern (Figure 7) suggest that the distance between nearest-neighbor molecules remains unchanged while distances between (micro)fibrils increases. Most likely this is caused by accumulation of an excess positive charge on collagen. Binding of dibasic phosphate neutralizes this charge, restores the diffraction pattern, and reduces the swelling.

"Free" Anions and Preferential Interactions. After all binding sites are occupied, further increase in the phosphate or sulfate concentration in the bathing solution leads to linear increase in the number of "free" interstitial anions not localized at any particular site (Figures 3 and 4). The slope of this dependence yields the partition coefficient $p < 1$ (Table 1), meaning that "free" anions are preferentially excluded from fibrils, that is, their net concentration in interstitial water is lower than that in the bath.

Our IR and X-ray data indicate that accumulation of bound and "free" interstitial anions is accompanied by displacement of water molecules and that the total interstitial volume inside fibrils remains unchanged within 0.5%. The IR spectra of "free" interstitial anions are closer to the bulk compared to those of bound anions but still downshifted by 3−6 cm^{-1} (Figure 2), indicating that their interactions with the immediate environment are still different from bulk water.

Most likely, "free" interstitial anions tend to accumulate at energetically favorable locations, for example, near positively charged side chains not involved in ion pairs. At the same time, they are preferentially excluded (displaced by water) from many unfavorable locations, for example, near hydrophobic or negatively charged side chains. Such relatively weak interactions of a protein with solutes vs water are traditionally referred to as "preferential interactions" (e.g., for detailed reviews, see refs *17*−*19*, *21*, and *22*). Their thermodynamic consequences depend only on the net interaction. In other words, although some sites on collagen may preferentially attract phosphate or sulfate, it is the net exclusion (*surface deficit*) of these anions from interstitial water in fibrils and water at collagen surface in solution that should affect fibrillogenesis thermodynamics. (Note that all interstitial water in fibrils is essentially surface water since surface-to-surface separation between collagen molecules in fibrils does not exceed 5−7 Å).

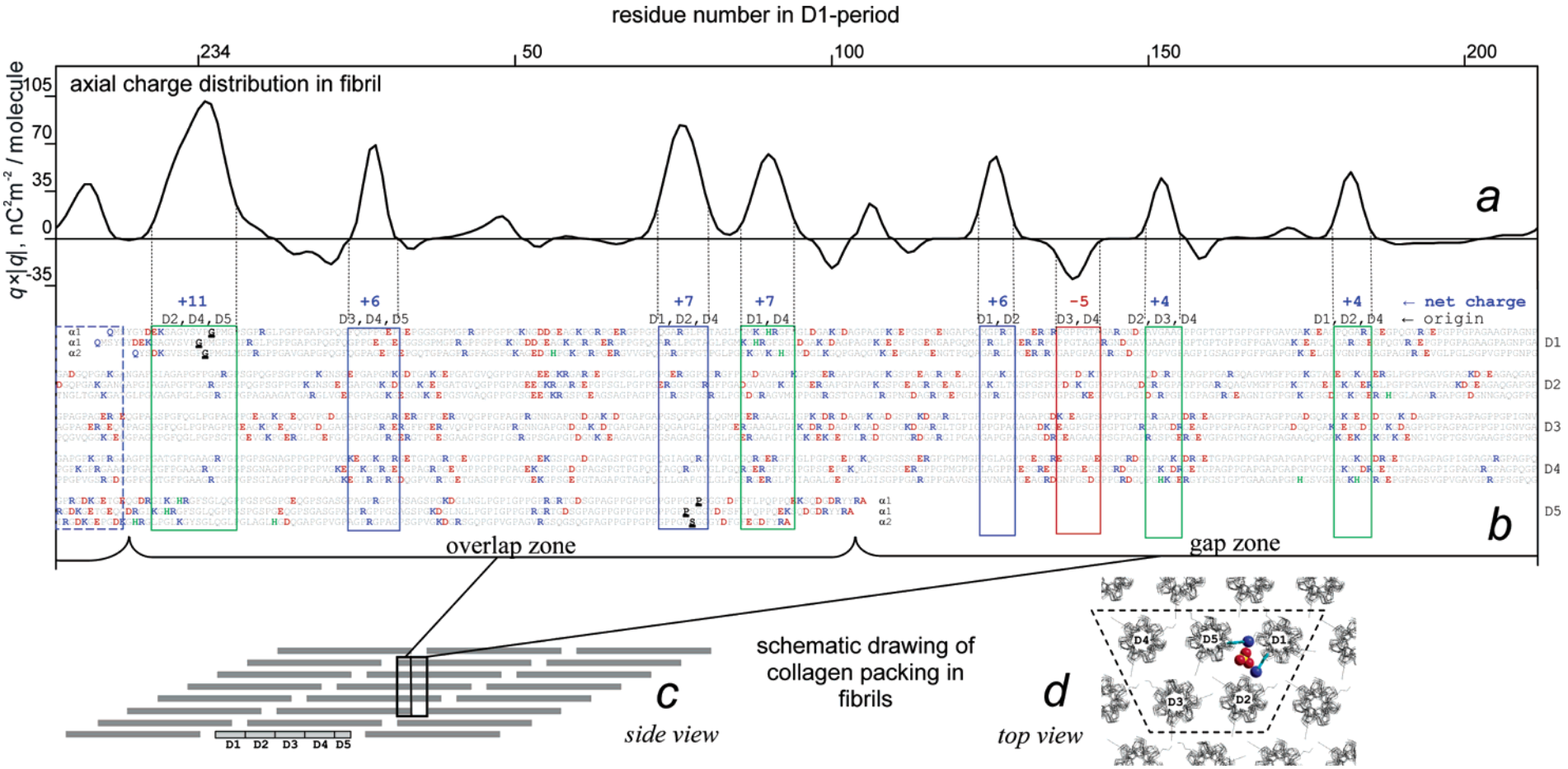

FIGURE 8: The pattern of axial charge density q in type I collagen fibrils (a) and potential sites for binding of multivalent ions (b). We assume that binding involves formation of salt bridges (d) between positively charged residues. Proposed locations of potential binding sites for anions (blue and green boxes) and cations (red box) correspond to the peaks in $q|q|$. These are regions of high excess axial charge density q with the largest probability ($\propto q^2$) of two unbalanced, like-charged residues to be close enough to form a salt bridge with a divalent counterion. (Due to ~8 Å length and high flexibility of charged side chains, phosphate and sulfate anions can bridge them even when the corresponding C_α-atoms are located ~22 Å away from each other). The axial alignment of charged residues is based on amino acid sequence of mouse collagen, 234-residue *D*-periodic stagger (c) of molecules in fibrils (*9*, *37*), and α1α2α1 register of the peptide α-chains within each molecule (*38*). The boxes containing titratable histidine residues are marked by green color. Net charge within each box (excess charge per five collagen molecules) is shown above the box. *D*-periods contributing the largest excess charge are listed under the net value. For simplicity, the *D*-periods are shown in panels b and d in a sequential order (*9*) (net axial charge density in a fibril does not depend on lateral arrangement of molecules). The first and last residues of the triple helix are marked black and underlined; positively charged residues are blue (all arginine, lysisne, and N-termini); negatively charged residues are red (aspartic acid, glutamic acid, and C-termini); histidine residues are green. The net charge density q per unit length of collagen molecule in the fibril was calculated as follows: Oppositely charged adjacent residues on the same chain were assumed to form an ion pair and were excluded. The density of the remaining charges was convoluted using a Gaussian window of seven residues (~20 Å) width at half-height (the maximal axial separation between C_α-atoms on two molecules at which like-charged side chains can form a direct salt bridge via a divalent counterion). Other convolution functions, alignments based on 233-residue stagger (*39*, *40*), and other chain registers, and different mammalian sequences produced similar charge patterns. Regions with the net charge of less than 3 were not marked. The dashed box indicates the region that might have a large positive excess charge but of which the charge is uncertain due to unknown conformation of nonhelical telopeptides.

Effect of Preferential Interactions on Critical Fibrillogenesis Concentration. To clarify the role of preferential interactions in fibrillogenesis, we revisited the dependence of collagen solubility (critical fibrillogenesis concentration) at 32 °C on phosphate and sulfate concentrations. As reported previously (*7*), the logarithm of collagen solubility increases almost linearly with the anion concentration in the 0−50 mM range (Figure 6). Such linearity is characteristic for preferential interactions (*17*, *18*). But, protein solubility is often expected to be decreased by excluded solutes because aggregation is assumed to reduce their surface deficit (by reducing the volume of water inaccessible to them). This argument does not apply to collagen the fibrils of which contain ∼55% of interstitial water and might exclude more anions than collagen solvation shells in solution. For instance, we can explain our observations by a modest 10−20% *increase* in the surface deficit of anions upon fibril formation.

In addition, Coulomb interactions between ions in the bathing solution might be substantially different from interactions between "free" ions in interstitial water inside collagen fibrils due to changes in dielectric properties of their immediate environment. This difference might result in a significant electrostatic contribution to preferential interactions. However, due to inherent difficulties in application of dielectric theories at nanometer distances and our lack of knowledge of microscopic dielectric properties of water, even a qualitative prediction of the sign of this contribution might be unreliable.

Overall, the observed increase in the critical fibrillogenesis concentration at 10−50 mM phosphate and sulfate appears to be related primarily to preferential interactions of these anions with collagen rather than binding. Monobasic phosphate does not appear to have any effect at 130 mM NaCl, while dibasic phosphate and sulfate have virtually identical effects. The observed pH dependence of the phosphate effect appears to be related to the variation in the concentration of dibasic phosphate ($pK_2 \approx 7$). The reported pH dependence of fibrillogenesis kinetics in phosphate buffers (*1*, *33*) might also have the same origin, but kinetic data are more difficult to interpret.

Comparison with Previous Studies. The ability of phosphate and sulfate anions to bind to collagen has been discussed in the literature for several decades. However, to the best of our knowledge, systematic measurements of the corresponding K_D, pH dependence, and discrimination of dibasic and monobasic forms of bound phosphate have not been reported. Therefore, we can compare our data only to the previously reported numbers of bound anions. Specifically, ∼25 bound phosphates per collagen molecule in the absence of NaCl were reported for calf-skin collagen at pH 7.4 (*5*). Similarly, ∼25 binding sites at low NaCl and ∼6 sites at 100 mM NaCl can be deduced from the measured (*34*) concentration dependence of total interstitial phosphate in rat-skin collagen at pH 7.2. Considering that these reports were based on chemical determination of phosphate concentration in fibers (*5*) or equilibration buffers (*34*) separated by centrifugation, the agreement of these values with our data is reasonable. In another study, ∼150 bound phosphates at 165 mM KCl/10 mM phosphate, pH 7.4, were reported for guinea-pig and carp collagens (*4*). However, this number of bound anions increased nearly linearly up to 10 mM phosphate (the highest concentration used in that study). If this were true binding, the linearity would mean that the observed 150 anions occupy less than half of all available binding sites and, therefore, that the number of binding sites exceeds ∼300 per molecule. In our opinion, this is unlikely since a collagen molecule has only 270−275 positively charged amino acid residues and most of them form ion pairs with neighboring negatively charged residues.

Phosphate and sulfate effects on the kinetics of collagen fibrillogenesis and the critical fibrillogenesis concentration have also been discussed. However, the mechanisms of the observed anion effects (*1*, *7*, *35*, *36*) and possible origins of the nontrivial pH dependence for phosphate effects (*33*) remained unclear. Most often it was presumed that the observed changes in fibrillogenesis kinetics were caused by phosphate or sulfate binding (*35*, *36*). For instance, it was proposed that phosphate could inhibit fibril formation by forming salt bridges between molecules in solution, thereby hindering proper alignment of molecules required for fibril formation (*35*). In contrast, we find that binding of divalent anions has a weak promoting rather than inhibiting effect on fibrillogenesis, that is, it reduces the critical fibrillogenesis concentration. We demonstrate that the observed net inhibition of fibrillogenesis is caused by stronger preferential exclusion of phosphate and sulfate from interstitial water in fibrils than from collagen hydration layers in solution. We also find that the differences in the effects of phosphate and sulfate reported before (*6*, *35*) were likely associated with mixed ionic composition of phosphate (divalent and monovalent) at neutral pH rather than by inherent differences in the effects of divalent anions.

CONCLUSIONS

Sulfate and phosphate bind to collagen at specific sites inside fibrils. At the same time, most anions not bound to these sites are preferentially excluded from interstitial water in fibrils.

At physiological conditions, there are one to two binding sites for sulfate and dibasic phosphate per collagen molecule inside fibrils. The dissociation constant for these sites at pH 6.8 is $K_D \approx 2$ mM. It decreases at lower and increases at higher pH. Bound divalent anions appear to form salt bridges between pairs of positively charged amino acid residues. The number of binding sites increases to ∼10 and the dissociation constant decreases 30−100 fold at low NaCl concentrations.

Divalent anion binding has weak promoting effect on collagen fibril formation. The increase in critical fibrillogenesis concentration (collagen solubility) observed at physiological NaCl appears to be caused primarily by the preferential exclusion of nonbound divalent anions (which makes fibril formation less thermodynamically favorable).

Unlike its divalent counterpart, monobasic phosphate exhibits no appreciable binding to collagen. It is excluded from interstitial water in fibrils almost as strongly as dibasic phosphate, but this has no effect on fibrillogenesis.

REFERENCES

1. Williams, B. R., Gelman, R. A., Poppke, D. C., and Piez, K. A. (1978) Collagen fibril formation. Optimal in vitro conditions and preliminary kinetic results, *J. Biol. Chem. 253*, 6578−6585.
2. Pogany, G., Hernandez, D. J., and Vogel, K. G. (1994) The in vitro interaction of proteoglycans with type I collagen is modulated by phosphate, *Arch. Biochem. Biophys. 313*, 102−111.

3. Thompson, J. B., Kindt, J. H., Drake, B., Hansma, H. G., Morse, D. E., and Hansma, P. K. (2001) Bone indentation recovery time correlates with bond reforming time, *Nature 414*, 773−776.
4. Glimcher, M. J., and Krane, S. M. (1964) The Incorporation of Radioactive Inorganic Orthophosphate as Organic Phosphate by Collagen Fibrils in Vitro, *Biochemistry 3*, 195−202.
5. Weinstok, A., King, P. C., and Wuthier, R. E. (1967) The Ion-Binding Characteristics of Reconstituted Collagen, *Biochem. J. 102*, 983−988.
6. Bensusan, H. B., and Hoyt B. L. (1958) The effect of various paramters on the rate of formation of fibers from collagen solutions, *J. Am. Chem. Soc. 58*, 719−724.
7. Kuznetsova, N., Chi, S. L., and Leikin, S. (1998) Sugars and polyols inhibit fibrillogenesis of type I collagen by disrupting hydrogen-bonded water bridges between the helices, *Biochemistry 37*, 11888−11895.
8. Griffiths, P. R., and de Haseth, J. A. (1986) in *Fourier Transform Infrared Spectroscopy* (Elving, P. J., and Winefordner, J. D., Eds.) pp 350−353, John Wiley and Sons, New York, Chichester, Brisbane, Toronto, Singapore.
9. Wess, T. J., Hammersley, A. P., Wess, L., and Miller, A. (1998) A consensus model for molecular packing of type I collagen, *J. Struct. Biol. 122*, 92−100.
10. Smith, J. W. (1968) Molecular packing in native collagen, *Nature 219*, 157−158.
11. Leikin, S., Parsegian, V. A., Yang, W., and Walrafen, G. E. (1997) Raman spectral evidence for hydration forces between collagen triple helices, *Proc. Natl. Acad. Sci. U.S.A. 94*, 11312−11317.
12. Nomura, S., Hiltner, A., Lando, J. B., and Baer, E. (1977) Interaction of water with native collagen, *Biopolymers 16*, 231−246.
13. Sasaki, N., Shiwa, S., Yagihara, S., and Hikichi, K. (1983) X-ray diffraction studies on the structure of hydrated collagen, *Biopolymers 22*, 2539−2547.
14. Mudd, C. P., Tipton, H., Parsegian, V. A., and Rau, D. C. (1987) Temperature-controlled vacuum chamber for X-ray diffraction studies, *Rev. Sci. Instrum. 58*, 2110−2114.
15. Kuznetsova, N. V., Forlino, A., Cabral, W. A., Marini, J. C., and Leikin, S. (2004) Structure, stability and interactions of type I collagen with GLY349−CYS substitution in α1(I) chain in a murine Osteogenesis Imperfecta model, *Matrix Biol. 23*, 101−112.
16. Schellman, J. A. (1987) Selective binding and solvent denaturation, *Biopolymers 26*, 549−559.
17. Timasheff, S. N., and Arakawa, T. (1988) Mechanism of Protein Precipitation and Stabilization by Co-Solvents, *J. Cryst. Growth 90*, 39−46.
18. Timasheff, S. N. (1993) The control of protein stability and association by weak interactions with water: how do solvents affect these processes? *Annu. Rev. Biophys. Biomol. Struct. 22*, 67−97.
19. Schellman, J. A. (1993) The Relation between the Free-Energy of Interaction and Binding, *Biophys. Chem. 45*, 273−279.
20. Anderson, C. F., Felitsky, D. J., Hong, J., and Record, M. T. (2002) Generalized derivation of an exact relationship linking different coefficients that characterize thermodynamic effects of preferential interactions, *Biophys. Chem. 101−102*, 497−511.
21. Record, M. T., Zhang, W. T., and Anderson, C. F. (1998) Analysis of effects of salts and uncharged solutes on protein and nucleic acid equilibria and processes: A practical guide to recognizing and interpreting polyelectrolyte effects, Hofmeister effects, and osmotic effects of salts, *Adv. Protein Chem. 51*, 281−353.
22. Wyman, J., and Gill, S. J. (1990) *Binding and linkage. Functional chemistry of biological macromolecules*, University Science Books, Mill Valley, CA.
23. Susi, H., Ard, J. S., and Carroll, R. J. (1971) The infrared spectrum and water binding of collagen as a function of relative humidity, *Biopolymers 10*, 1597−1604.
24. Leikin, S., Rau, D. C., and Parsegian, V. A. (1994) Direct measurement of forces between self-assembled proteins: temperature-dependent exponential forces between collagen triple helices, *Proc. Natl. Acad. Sci. U.S.A. 91*, 276−280.
25. Leikin, S., Rau, D. C., and Parsegian, V. A. (1995) Temperature-favoured assembly of collagen is driven by hydrophilic not hydrophobic interactions, *Nat. Struct. Biol. 2*, 205−210.
26. Kuznetsova, N., McBride, D. J., Jr., and Leikin, S. (2001) Osteogenesis imperfecta murine: interaction between type I collagen homotrimers, *J. Mol. Biol. 309*, 807−815.
27. Kadler, K. E., Hojima, Y., and Prockop, D. J. (1987) Assembly of collagen fibrils de novo by cleavage of the type I pC-collagen with procollagen C-proteinase. Assay of critical concentration demonstrates that collagen self-assembly is a classical example of an entropy-driven process, *J. Biol. Chem. 262*, 15696−15701.
28. Na, G. C., Phillips, L. J., and Freire, E. I. (1989) In vitro collagen fibril assembly: thermodynamic studies, *Biochemistry 28*, 7153−7161.
29. Eikenberry, E. F., and Brodsky, B. (1980) X-ray diffraction of reconstituted collagen fibers, *J. Mol. Biol. 144*, 397−404.
30. Brodsky, B., and Eikenberry, E. F. (1982) Characterization of fibrous forms of collagen, *Methods Enzymol. 82*, 127−174.
31. Hulmes, D. J. S., Wess, T. J., Prockop, D. J., and Fratzl, P. (1995) Radial packing, order, and disorder in collagen fibrils, *Biophys. J. 68*, 1661−1670.
32. San Antonio, J. D., Lander, A. D., Karnovsky, M. J., and Slayter, H. S. (1994) Mapping the heparin-binding sites on type I collagen monomers and fibrils, *J. Cell Biol. 125*, 1179−1188.
33. Veis, A., and Payne, K. (1988) Collagen fibrillogenesis, in *Collagen* (Nimni, M. E., Ed.) pp 113−137, CRC Press, Boca Raton, FL.
34. Nemeth-Csoka, M. (1977) The influence of inorganic phosphate and citrate anions on the effect of glycosaminoglycans during collagen fibril-formation, *Exp. Pathol. (Jena) 14*, 40−54.
35. Bensusan, H. B. (1960) Fiber formation from solutions of collagen. III. Some effects of environment on the rate of fiber formation. *J. Am. Chem. Soc. 82*, 4995−4998.
36. Nemeth-Csoka, M., and Tasnadi, G. (1981) The effect of inorganic pyrophosphate (PPi) anions on the in vitro collagen fibril formation, *Exp. Pathol. 20*, 58−63.
37. Hulmes, D. J., Miller, A., White, S. W., and Doyle, B. B. (1977) Interpretation of the meridional X-ray diffraction pattern from collagen fibres in terms of the known amino acid sequence, *J. Mol. Biol. 110*, 643−666.
38. Hofmann, H., Fietzek, P. P., and Kuhn, K. (1978) The role of polar and hydrophobic interactions for the molecular packing of type I collagen: a three-dimensional evaluation of the amino acid sequence, *J. Mol. Biol. 125*, 137−165.
39. Chapman, J. A., and Hardcastle, R. A. (1974) The staining pattern of collagen fibrils. II. A comparison with patterns computer-generated from the amino acid sequence, *Connect. Tissue Res. 2*, 151−159.
40. Chapman, J. A. (1974) The staining pattern of collagen fibrils. I. An analysis of electron micrographs, *Connect. Tissue Res. 2*, 137−150.

BI048788B